Eur. Phys. J. C (2019) 79:589
https://doi.org/10.1140/epjc/s10052-019-7100-1

THE EUROPEAN PHYSICAL JOURNAL C

Regular Article - Theoretical Physics

Extracting jet transport coefficient via single hadron and dihadron productions in high-energy heavy-ion collisions

Man Xie[1,a], **Shu-Yi Wei**[1,2,b], **Guang-You Qin**[1,c], **Han-Zhong Zhang**[1,d]

[1] Key Laboratory of Quark and Lepton Physics (MOE) and Institute of Particle Physics, Central China Normal University, Wuhan 430079, China
[2] Centre de Physique Théorique, Ecole Polytechnique, CNRS, Université Paris-Saclay, Route de Saclay, 91128 Palaiseau, France

Received: 19 January 2019 / Accepted: 2 July 2019 / Published online: 12 July 2019

Abstract We study the suppressions of high transverse momentum single hadron and dihadron productions in high-energy heavy-ion collisions based on the framework of a next-to-leading-order perturbative QCD parton model combined with the higher-twist energy loss formalism. Our model can provide a consistent description for the nuclear modification factors of single hadron and dihadron productions in central and non-central nucleus–nucleus collisions at RHIC and the LHC energies. We quantitatively extract the value of jet quenching parameter $\hat{q}$ via a global χ^2 analysis, and obtain $\hat{q}/T^3 = 4.1$–4.4 at $T = 378$ MeV at RHIC and $\hat{q}/T^3 = 2.6$–3.3 at $T = 486$ MeV at the LHC, which are consistent with the results from JET Collaboration. We also provide the predictions for the nuclear modification factors of dihadron productions in Pb + Pb collisions at $\sqrt{s_{\rm NN}} = 5.02$ TeV and in Xe + Xe collisions at $\sqrt{s_{\rm NN}} = 5.44$ TeV.

1 Introduction

The strongly-interacting quark–gluon plasma (QGP) can be created in high-energy heavy-ion collisions performed at the Large Hadron Collider (LHC) and the Relativistic Heavy-Ion Collider (RHIC). Jet quenching [1–3] has been regarded as an extremely useful tool for studying the properties of such hot and dense nuclear matter. When hard quarks or gluons traverse the QGP matter, they interact with the medium via multiple scatterings and medium-induced gluon radiations. The elastic and inelastic interactions between jet and medium may cause the energy loss of hard jet and also change the energy distribution among jet partons. As one of the consequences of jet quenching and energy loss, the yield of high transverse momentum hadrons fragmented from the surviving hard partons is suppressed as compared to that in proton–proton collisions normalized by the number of binary nucleon-nucleon collisions. Phenomenological studies have been performed on various jet quenching observables, such as the nuclear modifications of single hadron productions [4–8], dihadron and photon–hadron correlations [9–15], as well as the observables related to fully reconstructed jets in relativistic nuclear collisions [16–23].

In recent years, jet quenching studies have entered the quantitative era in that much effort has been devoted to the quantitative extraction of the so-called jet quenching parameter $\hat{q}$. This parameter is defined as the transverse momentum squared per unit length exchanged between the propagating hard parton and the traversed medium, $\hat{q} = d\langle(\Delta p_T)^2\rangle/dt$, and may be directly related to the gluon density of the nuclear medium [24]. Jet transport parameter $\hat{q}$ also controls the amount of medium-induced gluon radiation and thus radiative jet energy loss [24–29]. In addition, the transverse momentum broadening effect as controlled by $\hat{q}$ may lead to significant nuclear modification on back-to-back dijet, dihadron and other jet-related angular correlations [14,15]. Among many quantitative jet quenching studies, one of the most important steps is performed by JET Collaboration in Ref. [6] which has compared five different theoretical jet quenching models with the nuclear modification data on single hadron productions in most central collisions at RHIC and the LHC and quantitatively extracted the temperature dependence of jet quenching parameter $\hat{q}$. The values of $\hat{q}$ temperatures available at RHIC and the LHC have been obtained as: $\hat{q}/T^3 = 4.6 \pm 1.2$ at $T \approx 370$ MeV and $\hat{q}/T^3 = 3.7 \pm 1.4$ at $T \approx 470$ MeV for a 10 GeV quark jet [30]. Following this direction, Refs. [30–32] have studied the centrality and collision energy dependence of $\hat{q}$ values at both RHIC and the LHC. Also, Ref. [14] has utilized the nuclear modification data on back-to-back dihadron and hadron-jet angular correlations to extract the value of $\hat{q}$ at RHIC.

[a] e-mail: 724712536@qq.com
[b] e-mail: weishuyi.sdu@gmail.com
[c] e-mail: guangyou.qin@mail.ccnu.edu.cn
[d] e-mail: zhanghz@mail.ccnu.edu.cn

This paper follows closely the above efforts and study the nuclear modifications of both single hadron and dihadron productions at high transverse momenta using a next-to-leading-order (NLO) perturbative QCD model combined with the higher-twist energy loss formalism. In particular, we perform a global χ^2 analysis on the nuclear modification data on single hadron and dihadron productions at RHIC [33–36] and the LHC [37–45] and quantitatively extract the values of jet quenching parameter $\hat{q}$. Our analysis yields $\hat{q}/T^3 = 4.1$–4.4 at $T = 378$ MeV at RHIC and $\hat{q}/T^3 = 2.6$–3.3 at $T = 486$ MeV at the LHC. These results are quantitatively consistent with JET Collaboration. We also extract the $\hat{q}$ values for Pb+Pb collisions at $\sqrt{s_{\rm NN}} = 5.02$ TeV and Xe+Xe collisions at $\sqrt{s_{\rm NN}} = 5.44$ TeV using the single hadron nuclear modification data, and predict the nuclear modification factors for dihadron productions for these collisions.

Our paper is organized as follows. In Sect. 2, we briefly introduce our framework to study the productions of single hadrons and dihadrons at high transverse momenta in proton–proton and nucleus–nucleus collisions. In Sect. 3, we perform a global χ^2 analysis and extract jet quenching parameter $\hat{q}$ from the nuclear modification data on single hadron and dihadron productions at RHIC and the LHC. We also provide our predictions for the nuclear modification factors of dihadron productions in central and non-central Pb+Pb collisions at $\sqrt{s_{\rm NN}} = 5.02$ TeV and Xe+Xe collisions at $\sqrt{s_{\rm NN}} = 5.44$ TeV at the LHC. Sect. 4 contains our summary.

2 Framework

In high-energy proton–proton collisions, the production cross section of high transverse momentum hadrons can be factorized into a convolution of parton distribution functions (PDFs), the cross section of hard partonic scatterings, and fragmentation functions (FFs),

$$\frac{d\sigma^h_{pp}}{dyd^2p_T} = \sum_{abcd}\int dx_a dx_b f_{a/p}(x_a,\mu^2) f_{b/p}(x_b,\mu^2) \times\frac{1}{\pi}\frac{d\sigma_{ab\to cd}}{d\hat{t}}\frac{D^h_c(z_c,\mu^2)}{z_c} + \mathcal{O}(\alpha_s^3). \quad (1)$$

Here, $f_a(x_a,\mu^2)$ and $f_b(x_b,\mu^2)$ are parton distribution functions which we take from CT14 [46]; $D^h_c(z_c,\mu^2)$ is fragmentation function which we take from Refs. [47,48]; $d\sigma_{ab\to cd}/d\hat{t}$ is the tree-level $2\to 2$ partonic scattering cross section. The NLO correction at $\mathcal{O}(\alpha_s^3)$ contains $2\to 2$ virtual diagrams and $2\to 3$ tree diagrams, and has been included in our calculation. It has been shown in Ref. [9] that NLO perturbative QCD calculation for single π^0 production in proton–proton collisions agrees well with the experimental data at RHIC.

Similarly, the production cross section for high transverse momentum dihadrons in high-energy proton–proton collisions can be written as,

$$\frac{d\sigma^{h_1h_2}_{pp}}{dPS} = \sum_{abcd}\int \frac{dz_c}{z_c^2}\frac{dz_d}{z_d^2} x_a f_{a/p}(x_a,\mu^2) x_b f_{b/p}(x_b,\mu^2) \times\frac{1}{\pi}\frac{d\sigma_{ab\to cd}}{d\hat{t}} D^{h_1}_c(z_c,\mu^2) D^{h_2}_d(z_d,\mu^2) \times\delta^2\left(\frac{\vec{p}^{\,h_1}_T}{z_c}+\frac{\vec{p}^{\,h_2}_T}{z_d}\right) + \mathcal{O}(\alpha_s^3), \quad (2)$$

where the phase space is $dPS = dy^{h_1}d^2p_T^{h_1}dy^{h_2}d^2p_T^{h_2}$.

In relativistic nucleus–nucleus collisions, one has to consider both cold nuclear matter effect in the initial state and hot nuclear matter effect in the final state. The yield of single hadron production at high transverse momentum may be obtained as [9,10],

$$\frac{dN^h_{AB}}{dyd^2p_T} = \sum_{abcd}\int dx_a dx_b d^2r t_A(\vec{r}) t_B(\vec{r}+\vec{b}) \times f_{a/A}(x_a,\mu^2,\vec{r}) f_{b/B}(x_b,\mu^2,\vec{r}+\vec{b}) \times\frac{1}{\pi}\frac{d\sigma_{ab\to cd}}{d\hat{t}}\frac{\tilde{D}^h_c(z_c,\mu^2,\Delta E_c)}{z_c} + \mathcal{O}(\alpha_s^3). \quad (3)$$

Similarly, the yield of dihadron production at high transverse momentum in nucleus–nucleus collisions may be calculated as [9,10,49]

$$\frac{dN^{h_1h_2}_{AB}}{dPS} = \sum_{abcd}\int \frac{dz_c}{z_c^2}\frac{dz_d}{z_d^2} d^2r t_A(\vec{r}) t_B(\vec{r}+\vec{b}) \times x_a f_{a/A}(x_a,\mu^2,\vec{r}) x_b f_{b/B}(x_b,\mu^2,\vec{r}+\vec{b}) \times\frac{1}{\pi}\frac{d\sigma_{ab\to cd}}{d\hat{t}}\tilde{D}^{h_1}_c(z_c,\mu^2,\Delta E_c)\tilde{D}^{h_2}_d(z_d,\mu^2,\Delta E_d) \times\delta^2\left(\frac{\vec{p}^{\,h_1}_T}{z_c}+\frac{\vec{p}^{\,h_2}_T}{z_d}\right) + O(\alpha_s^3). \quad (4)$$

In the above two equations, $t_A(\vec{r})$ is the nuclear thickness function, normalized as $\int d^2r t_A(\vec{r}) = A$, with A the mass number of the nucleus. Here we use the Woods–Saxon form for the nuclear density distribution. $f_{a/A}(x_a,\mu^2,\vec{r})$ is the nuclear modified PDF, which we calculate as follows [50,51]:

$$f_{a/A}(x_a,\mu^2,\vec{r}) = S_{a/A}(x_a,\mu^2,\vec{r})\left[\frac{Z}{A}f_{a/p}(x_a,\mu^2) + \left(1-\frac{Z}{A}\right)f_{a/n}(x_a,\mu^2)\right], \quad (5)$$

where Z is the proton number of the nucleus. Here, $S_{a/A}(x_a,\mu^2,\vec{r})$ is called the nuclear shadowing factor and denotes the nuclear modification to the PDF in a free proton $f_{a/p}(x_a,\mu^2)$. The shadowing factor $S_{a/A}(x_a,\mu^2,\vec{r})$ is calculated using the following form [52,53],

$$S_{a/A}(x_a,\mu^2,\vec{r}) = 1 + [S_{a/A}(x_a,\mu^2) - 1]\frac{At_A(\vec{r})}{\int d^2r[t_A(\vec{r})]^2}, \tag{6}$$

where $S_{a/A}(x_a,\mu^2)$ is taken from the EPPS16 [54]. $\tilde{D}_c^h(z_c,\Delta E_c)$ is the medium-modified fragmentation function and is calculated as follows [9,10,48]:

$$\begin{aligned}\tilde{D}_c^h(z_c,\mu^2,\Delta E_c) = (1-e^{-\langle N_g\rangle})\left[\frac{z_c'}{z_c}D_c^h(z_c',\mu^2)\right.\\ \left.+\langle N_g\rangle\frac{z_g{}'}{z_c}D_g^h(z_g{}',\mu^2)\right]\\ +e^{-\langle N_g\rangle}D_c^h(z_c,\mu^2),\end{aligned} \tag{7}$$

where ΔE_c is the energy loss of parton c, $z_c = p_T/p_{Tc}$, $z_c' = p_T/(p_{Tc}-\Delta E_c)$, $z_g' = \langle N_g\rangle p_T/\Delta E_c$ and $\langle N_g\rangle$ is the average number of gluons radiated by parton c. The above equation includes the effect of multiple gluon emissions assuming a Poisson distribution for the number of emitted gluons. The Poisson assumption has also been used in GLV and ASW models to construct the energy loss distribution [55,56]. Note that transport and DGLAP evolutions are the two other popular methods to resum multiple gluon emissions from single gluon emission kernel [28,57–59]. In this work, we use the higher twist formalism [28,60–62] to calculate medium-induced gluon radiation and parton energy loss. For a quark with initial energy E, the total energy loss ΔE can be calculated as,

$$\begin{aligned}\frac{\Delta E}{E} = \frac{2C_A\alpha_s}{\pi}\int d\tau\int\frac{dl_T^2}{l_T^4}\int dz\\ \times\left[1+(1-z)^2\right]\hat{q}\sin^2\left(\frac{l_T^2\tau}{4z(1-z)E}\right),\end{aligned} \tag{8}$$

where $C_A = 3$, and l_T is the transverse momentum of radiated gluon. We assume the energy loss of a gluon is simply 9/4 times that of a quark [60]. The average number of radiated gluons from the propagating hard parton is calculated as [63],

$$\begin{aligned}\langle N_g\rangle = \frac{2C_A\alpha_s}{\pi}\int d\tau\int\frac{dl_T^2}{l_T^4}\int\frac{dz}{z}\\ \times\left[1+(1-z)^2\right]\hat{q}\sin^2\left(\frac{l_T^2\tau}{4z(1-z)E}\right).\end{aligned} \tag{9}$$

The parton energy loss is controlled by jet transport parameter $\hat{q}$ [24], for which we take the following form:

$$\hat{q} = \hat{q}_0\frac{T^3}{T_0^3}\frac{p^\mu u^\mu}{p_0}, \tag{10}$$

where T is the local temperature of the medium, T_0 is a reference temperature which is usually taken as the temperature at the center of the medium at the hydrodynamics initial time $\tau_0 = 0.6$ fm in central nucleus–nucleus collisions, and u^μ is the four flow velocity of the fluid. In our calculation, the dynamical evolution of the QGP medium is obtained using the OSU (2+1)-dimensional viscous hydrodynamics model (VISH2+1) [64–67].

3 Numerical results

In this section, we present our numerical results for single hadron and dihadron nuclear modification factors in Au+Au collisions at $\sqrt{s_{\rm NN}} = 0.2$ TeV, Pb+Pb collisions at $\sqrt{s_{\rm NN}} = 2.76$ TeV and 5.02 TeV, and Xe+Xe collisions at $\sqrt{s_{\rm NN}} = 5.44$ TeV. A global χ^2 analysis is performed to extract the jet quenching parameter $\hat{q}$ in different collision systems and different collision energies at RHIC and the LHC. Based on our analysis, we also provide the predictions for the nuclear modification factors of dihadron productions in Pb+Pb collisions at $\sqrt{s_{\rm NN}} = 5.02$ TeV and Xe+Xe collisions at $\sqrt{s_{\rm NN}} = 5.44$ TeV.

The nuclear modification factor R_{AA} for single hadron production in heavy-ion collisions is defined as [48],

$$R_{AA} = \frac{dN_{AB}^h/dyd^2p_T}{\langle T_{AA}\rangle d\sigma_{pp}^h/dyd^2p_T}, \tag{11}$$

where $T_{AA}(\vec{b}) = \int d^2rt_A(\vec{r})t_B(\vec{r}+\vec{b})$ is the overlap function of two colliding nuclei and the average in the equation is taken for a given centrality class.

As for dihadron production at high transverse momentum in heavy-ion collisions, the nuclear modification factor I_{AA} can be defined either as a function of p_T^{assoc} or as a function of $z_T = p_T^{assoc}/p_T^{trig}$ [9]

$$\begin{aligned}I_{AA}(p_T^{assoc}) = \frac{D_{AA}(p_T^{assoc})}{D_{pp}(p_T^{assoc})},\\ I_{AA}(z_T) = \frac{D_{AA}(z_T)}{D_{pp}(z_T)},\end{aligned} \tag{12}$$

where $D_{AA}(z_T) = p_T^{trig}D_{AA}(p_T^{assoc})$ is called hadron-triggered fragmentation function [68],

$$D_{AA}(z_T) = p_T^{trig}\frac{dN_{AA}^{h_1h_2}/dy^{trig}dp_T^{trig}dy^{assoc}dp_T^{assoc}}{\langle T_{AA}\rangle d\sigma_{AA}^{h_1}/dy^{trig}dp_T^{trig}}. \tag{13}$$

3.1 Au+Au collisions at $\sqrt{s_{\rm NN}} = 0.2$ TeV at RHIC

Figure 1 shows our calculations for single hadron and dihadron nuclear modification factors in central (0–10%) Au+Au collisions at $\sqrt{s_{\rm NN}} = 0.2$ TeV at RHIC compared with the experimental data taken from PHENIX [33,34] and STAR [36] Collaborations. In each plot, different lines represent our model calculations for R_{AA} or I_{AA}

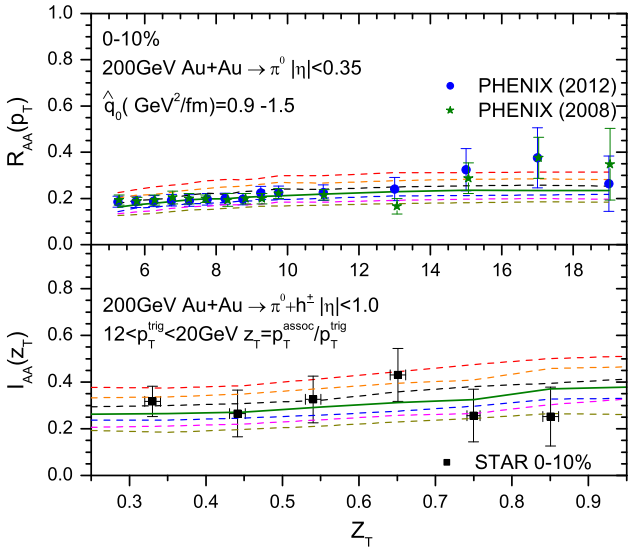

Fig. 1 The single hadron and dihadron suppression factors in central 0–10% Au + Au collisions at $\sqrt{s_{\rm NN}} = 0.2$ TeV compared with PHENIX [33,34] and STAR [36] data

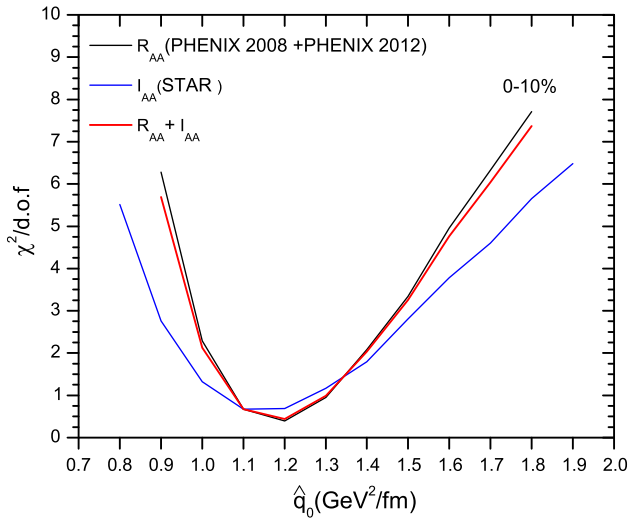

Fig. 2 Global χ^2 analysis for single hadron and (or) dihadron nuclear suppression factors in Au + Au collisions at $\sqrt{s_{\rm NN}} = 0.2$ TeV at RHIC

using different values of jet quenching parameter $\hat{q}_0$. The solid line in the middle denotes the result using the best value of $\hat{q}_0$ obtained from our global χ^2 analysis, which is shown in Fig. 2. Note that our χ^2 is defined as follows, $\chi^2 = \sum_{i=1}^{N} \left[(V_{\rm th} - V_{\rm exp})^2 / (\sigma_{\rm sys}^2 + \sigma_{\rm stat}^2) \right]$, where $V_{\rm exp}$ and $V_{\rm th}$ denote the experimental and theory values, and $\sigma_{\rm sys}$ and $\sigma_{\rm stat}$ represent systematic and statistical errors of the experimental data. In the figure, we also show χ^2/d.o.f as a function of $\hat{q}_0$ using only R_{AA} data or only I_{AA} data. We can see that two fitting results are consistent with each other. This means that with the similar value of $\hat{q}_0$, both single hadron and dihadron nuclear suppression factors can be described

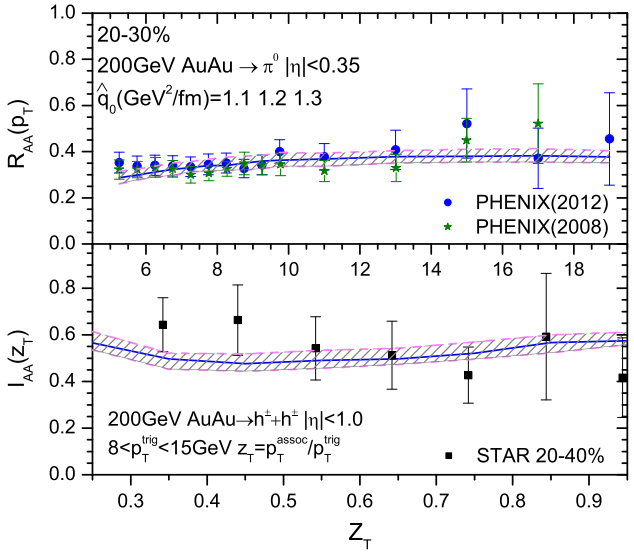

Fig. 3 The single hadron and dihadron suppression factors in mid-central Au + Au collisions at $\sqrt{s_{\rm NN}} = 0.2$ TeV compared with PHENIX [33,34] and STAR [35] data

consistently within our jet energy loss model. Our global χ^2 analysis renders: $\hat{q}_0 = 1.1$– $1.2\ {\rm GeV}^2/{\rm fm}$ at $T_0 = 378$ MeV. In terms of the scaled dimensionless jet quenching parameter, it reads, $\hat{q}/T^3 = 4.1$–4.4 at $T = 378$ MeV. These values are consistent with the results obtained by JET Collaboration [6].

To test the quality of our approach, we use the same $\hat{q}_0$ value obtained above to calculate the nuclear modification factors R_{AA} and I_{AA} in mid-central Au + Au collision at $\sqrt{s_{\rm NN}} = 0.2$ TeV at RHIC. The result is shown in Fig. 3, where the solid lines in the middle denote the results using the best $\hat{q}_0$ value (i.e, $\hat{q}_0 = 1.2\ {\rm GeV}^2/{\rm fm}$ at $T_0 = 378$ MeV), while the other two lines represent the uncertainty for the extracted $\hat{q}_0$ value ($\hat{q}_0 = 1.1$ or $1.3\ {\rm GeV}^2/{\rm fm}$ for the two lines). We can see that with the similar $\hat{q}_0$ value, our model can provide a good description of experimental data on single and dihadron nuclear modification in both central and non-central Au + Au collisions at $\sqrt{s_{\rm NN}} = 0.2$ TeV at RHIC.

3.2 Pb + Pb collisions at $\sqrt{s_{\rm NN}} = 2.76$ TeV at the LHC

Now we present our numerical results for Pb + Pb collisions at $\sqrt{s_{\rm NN}} = 2.76$ TeV at the LHC. Figure 4 shows our calculations for single hadron and dihadron nuclear modification factors in central (0–10%) Pb + Pb collisions at $\sqrt{s_{\rm NN}} = 2.76$ TeV compared with the experimental data from ALICE [37,43,44] and CMS [38,45] Collaborations. In each plot, different lines represent our model calculations for R_{AA} and (or) I_{AA} using different $\hat{q}_0$ values. The solid line in the middle denotes the results using the best $\hat{q}_0$ value obtained from our global χ^2 analysis. Also shown

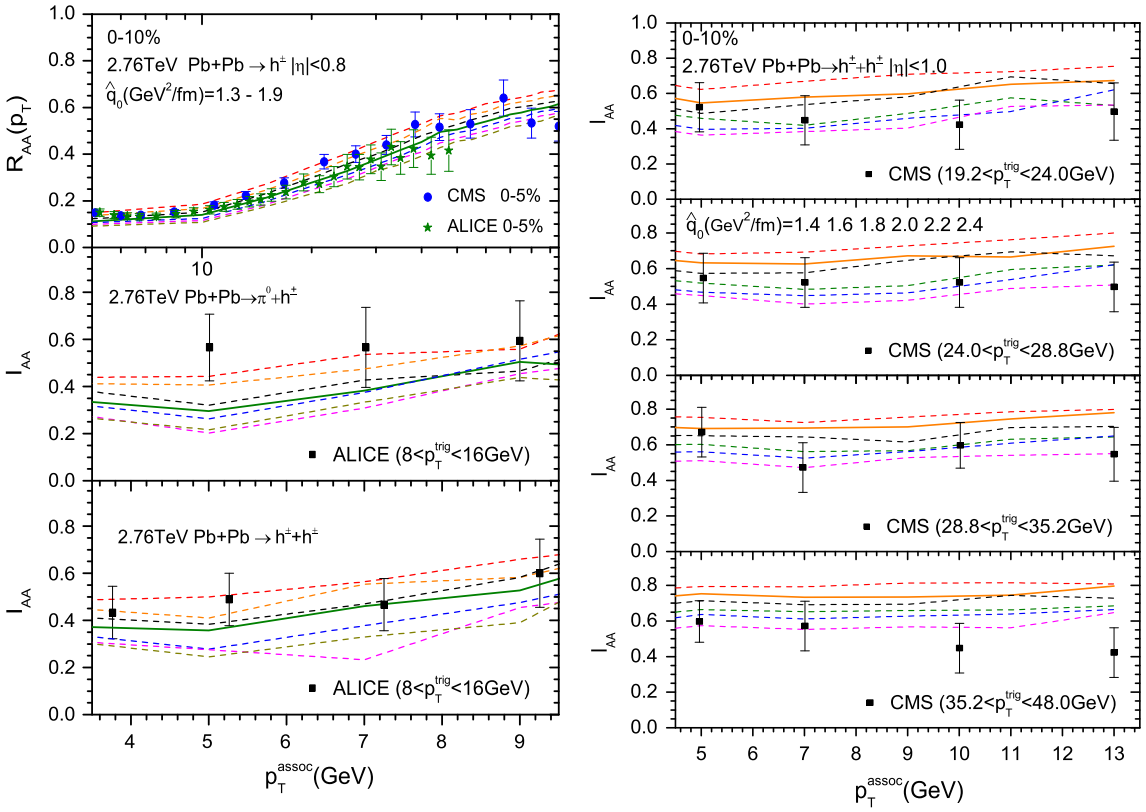

Fig. 4 The single hadron and dihadron suppression factors in 0–10% Pb+Pb collisions at $\sqrt{s_{\rm NN}} = 2.76$ TeV compared with CMS [38,45] and ALICE [37,43,44] data

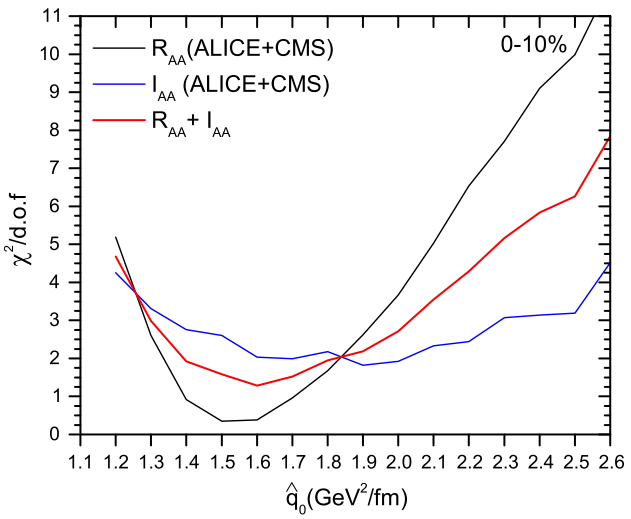

Fig. 5 Global χ^2 analysis for single hadron and (or) dihadron nuclear suppression factors in Pb+Pb collisions at $\sqrt{s_{\rm NN}} = 2.76$ TeV at the LHC

in Fig. 5 is the χ^2 analysis of $\hat{q}_0$ value using only R_{AA} data or I_{AA} data. Although there is some small difference between two fitting results, they are quantitatively consistent with each other within the uncertainties. Such consistency implies that with the similar values of $\hat{q}_0$, our jet energy loss model can provide a consistent description of both single hadron and dihadron nuclear suppression factors in Pb+Pb collisions at $\sqrt{s_{\rm NN}} = 2.76$ TeV. From Fig. 5, we obtain: $\hat{q}_0 = 1.5$–1.9 GeV^2/fm at $T_0 = 486$ MeV, which translates into the scaled jet quenching parameter, $\hat{q}/T^3 = 2.6$–3.3 at $T = 486$ MeV. This values are also consistent with JET Collaboration [6].

We also test our approach by using the same $\hat{q}_0$ value obtained above to calculate the nuclear modification factors R_{AA} and I_{AA} in the non-central (50–60%) Pb+Pb collisions at $\sqrt{s_{\rm NN}} = 2.76$ TeV. The result is shown in Fig. 6: the solid lines in the middle denote the results using the best $\hat{q}_0$ value (i.e., $\hat{q}_0 = 1.6$ GeV^2/fm at $T_0 = 486$ MeV), while the other two lines (using $\hat{q}_0 = 1.5$ and 1.9 GeV^2/fm) represent the uncertainty for our extracted $\hat{q}_0$ value. We can see that with the same $\hat{q}_0$ value, our jet energy loss model can also describe the experimental data on single and dihadron nuclear modification in non-central Pb+Pb collisions at $\sqrt{s_{\rm NN}} = 2.76$ TeV. Another interesting result is that for both Au+Au collisions at RHIC and Pb+Pb collision at the LHC, the nuclear modification factors I_{AA} for dihadron productions are typically larger than single hadron suppression factors R_{AA} given the same nucleus–nucleus collision conditions. As shown in Refs. [9,69,70], high p_T single hadrons mainly come from

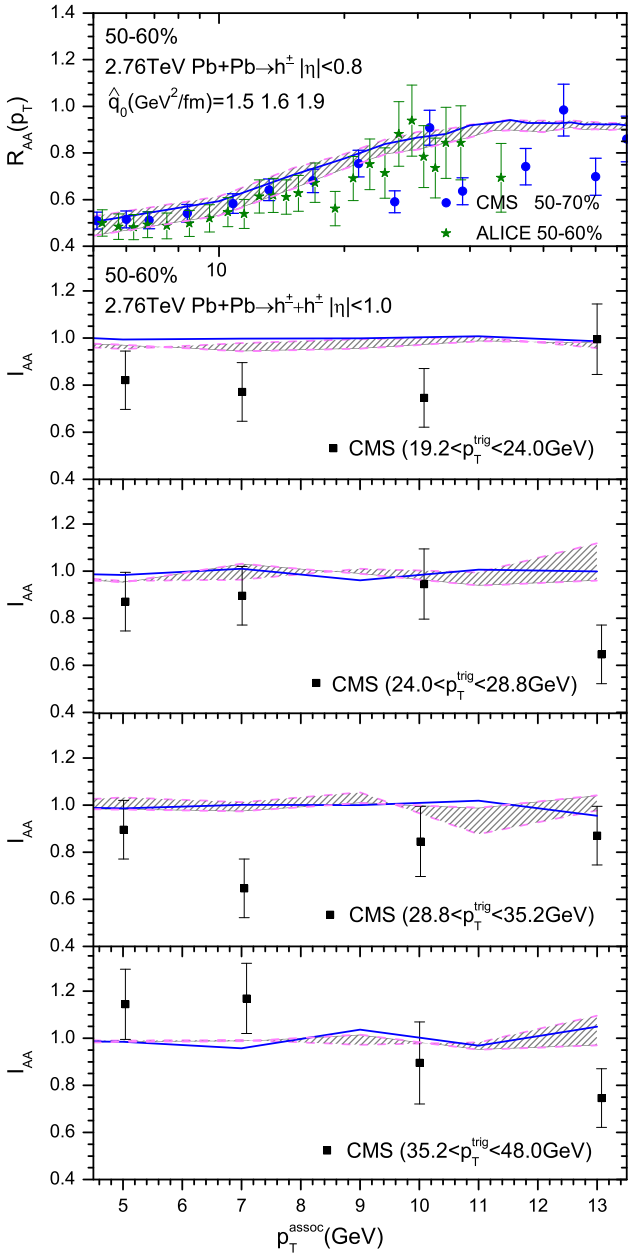

Fig. 6 The single hadron and dihadron suppression factors in non-central (50–60%) Pb+Pb collisions at $\sqrt{s_{\rm NN}} = 2.76$ TeV compared with ALICE [37] and CMS [38,45] data

jets that are initially produced in the outer corona of the overlap region (usually called surface bias emission), while high p_T dihadrons come from a combination of surfacial and tangential jets as well as punching-through jets. Surface bias means a large amount of jets produced at the central region of the medium lose most of their energies and do not contribute to final observed hadrons. On average in a $A + A$ event, since the total energy loss for jets in the surface bias case is larger than in the case with punching-through jets, typically $R_{AA} < I_{AA}$.

3.3 Pb+Pb collisions at $\sqrt{s_{\rm NN}} = 5.02$ TeV and Xe+Xe collisions at $\sqrt{s_{\rm NN}} = 5.44$ TeV at the LHC

Recently, ALICE [41,42] and CMS [39,40] Collaborations have published their measurements on the nuclear modification factor R_{AA} for single hadron productions in Pb+Pb collisions at $\sqrt{s_{\rm NN}} = 5.02$ TeV and Xe+Xe collisions at $\sqrt{s_{\rm NN}} = 5.44$ TeV. These new results provide a good opportunity for studying the collision energy and system size dependencies of jet quenching in relativistic heavy-ion collisions. Since no experimental data on dihadron nuclear modification factor I_{AA} are available for these collisions, we will extract the $\hat{q}_0$ values only using the available R_{AA} data. Given that our model can provide a consistent description of both single hadron and dihadron nuclear modifications in Au+Au collisions at $\sqrt{s_{\rm NN}} = 0.2$ TeV and Pb+Pb collisions at $\sqrt{s_{\rm NN}} = 2.76$ TeV, we then use the extracted $\hat{q}_0$ values to predict dihadron nuclear modification factor I_{AA} in Pb+Pb collisions at $\sqrt{s_{\rm NN}} = 5.02$ TeV and Xe+Xe collisions at $\sqrt{s_{\rm NN}} = 5.44$ TeV.

Our numerical results are shown in Figs. 7 and 8, in which the left panels show the result for Pb+Pb collisions at $\sqrt{s_{\rm NN}} = 5.02$ TeV and the right for Xe+Xe collisions at $\sqrt{s_{\rm NN}} = 5.44$ TeV. Figure 7 shows the nuclear modification factor R_{AA} (in the upper panels) together with the χ^2 analysis (in the lower panels). Again, the solid lines are the results using the best fit $\hat{q}_0$ values. From our χ^2 analysis, we obtain: $\hat{q}_0 \approx 1.7$ GeV^2/fm at $T_0 = 516$ MeV ($\hat{q}/T^3 \approx 2.5$) for central Pb+Pb collisions at $\sqrt{s_{\rm NN}} = 5.02$ TeV and $\hat{q}_0 \approx 1.8$ GeV^2/fm at $T_0 = 469$ MeV ($\hat{q}/T^3 \approx 3.5$) for central Xe+Xe collisions at $\sqrt{s_{\rm NN}} = 5.44$ TeV. Using the extracted $\hat{q}_0$ values from fitting R_{AA} data, we present in Fig. 8 our predictions for dihadron nuclear modification factor I_{AA} in central Pb+Pb collisions at $\sqrt{s_{\rm NN}} = 5.02$ TeV (left) and central Xe+Xe collisions at $\sqrt{s_{\rm NN}} = 5.44$ TeV (right). Different panels are the results with different transverse momenta for trigger hadrons. In each plot, the solid lines in the middle are the results using the best $\hat{q}_0$ values, while the other two lines represent the theoretical which we take ± 0.1 GeV^2/fm around the best $\hat{q}_0$ values fitted from R_{AA} data. One interesting observation is that as the values of I_{AA} also increase as one increases the trigger hadron transverse momentum. Similar to why $R_{AA} < I_{AA}$, this can also be understood as follows. With increasing trigger hadron p_T, the contribution from punching-through jets increases (as shown in [69]), thus the average total energy loss of jets decreases, which explains why I_{AA} increases with increasing hadron p_T.

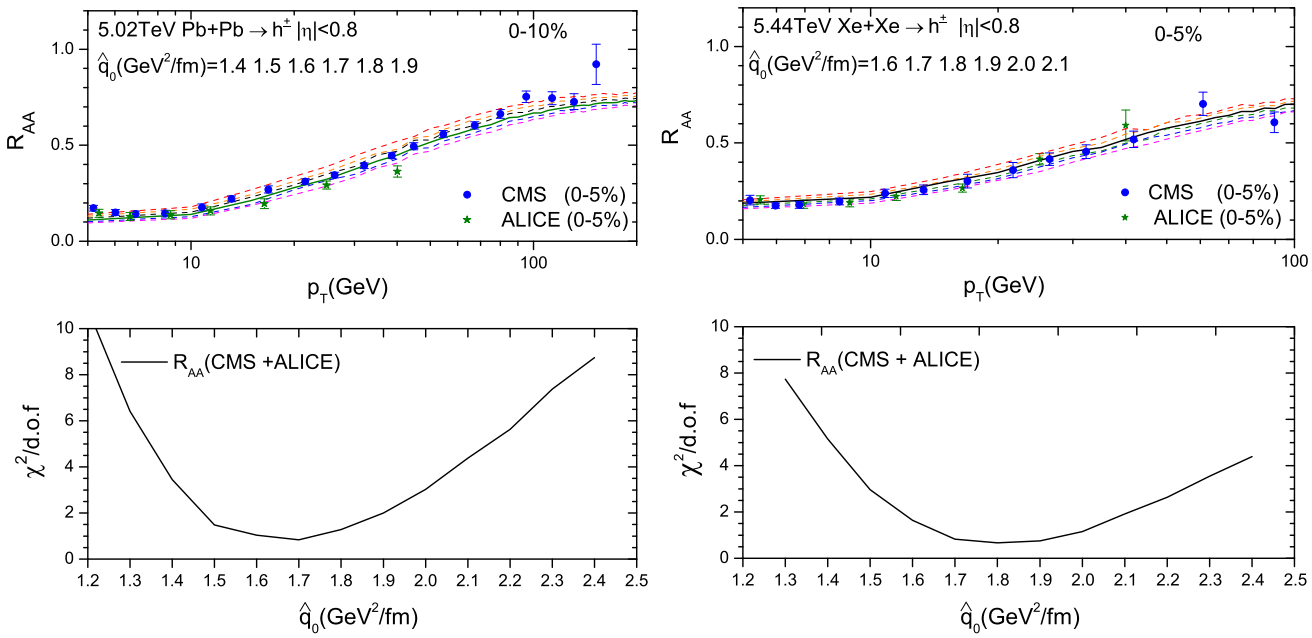

Fig. 7 The single hadron suppression factors in central Pb + Pb collisions at $\sqrt{s_{\rm NN}} = 5.02$ TeV and in central Xe + Xe collisions at $\sqrt{s_{\rm NN}} = 5.44$ TeV compared with CMS [39,40] and ALICE [41,42] data

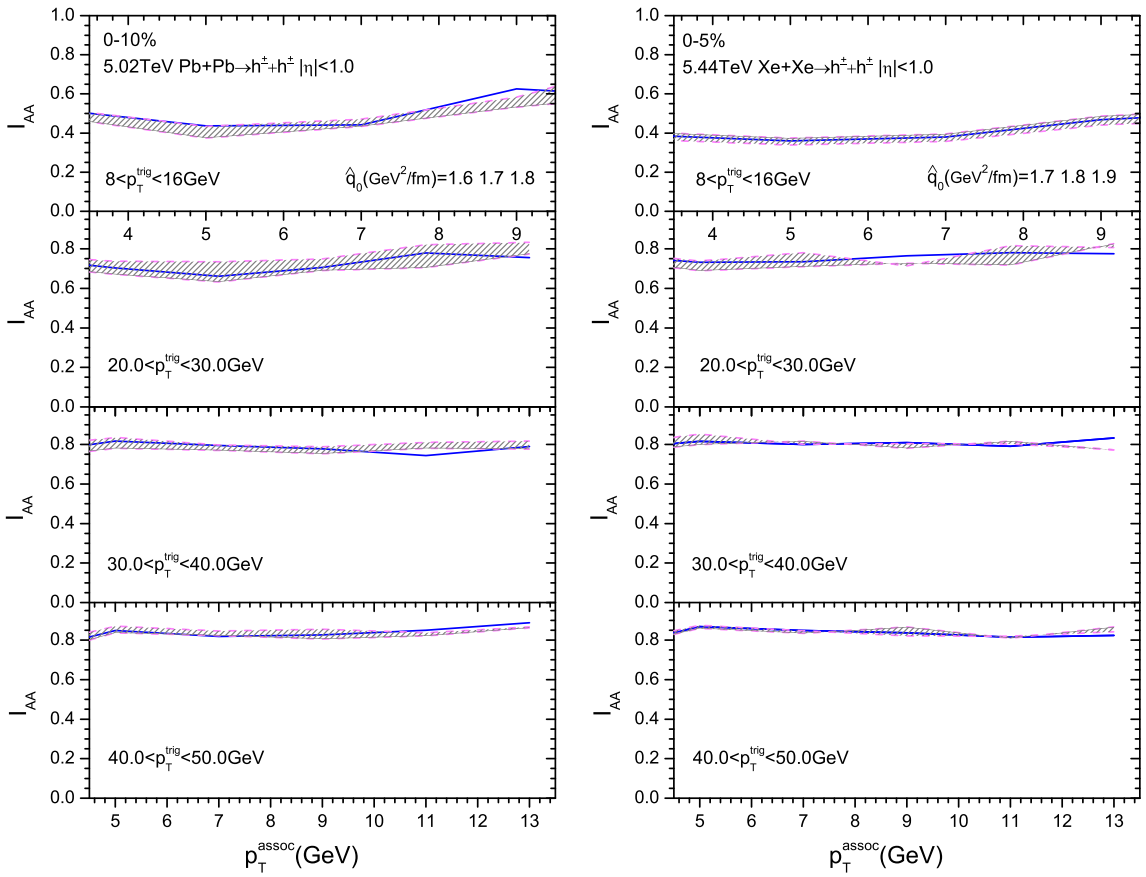

Fig. 8 The predictions of dihadron suppression factors in central Pb + Pb collisions at $\sqrt{s_{\rm NN}} = 5.02$ TeV and in central Xe + Xe collisions at $\sqrt{s_{\rm NN}} = 5.44$ TeV

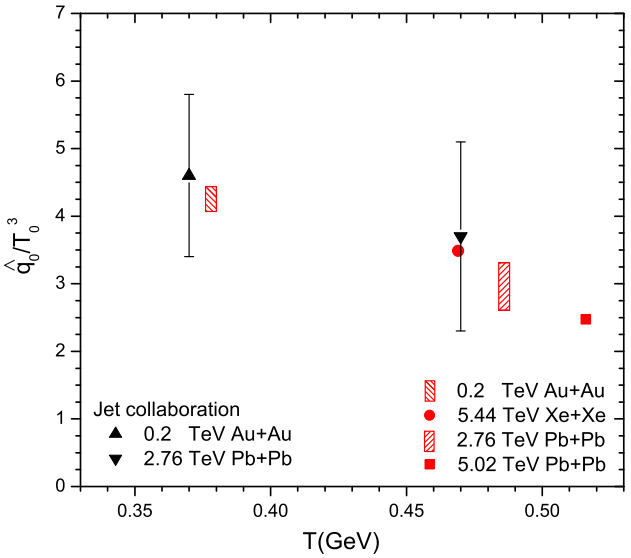

Fig. 9 The scaled jet quenching parameter $\hat{q}/T^3$ extracted via single hadron and dihadron suppression data at RHIC and the LHC. The boxes are Jet Collaboration results

3.4 $\hat{q}$ from single hadron and dihadron nuclear suppressions at RHIC and the LHC

In previous subsections, we have quantitatively extracted the jet quenching parameter $\hat{q}$ by performing a detailed χ^2 analysis on the comparison of our jet energy loss model calculations to single hadron and dihadron nuclear modification data at RHIC and the LHC. Here we summarize the main results for the extracted $\hat{q}$ values, in terms of the scaled jet quenching parameter $\hat{q}/T^3$:

$$\begin{aligned}
\frac{\hat{q}}{T^3} &= 4.1\text{–}4.4, \quad T = 378\ \text{MeV}, \text{Au} + \text{Au}\ 0.2\text{A TeV};\\
\frac{\hat{q}}{T^3} &= 3.5, \qquad\quad T = 469\ \text{MeV}, \text{Xe} + \text{Xe}\ 5.44\text{A TeV};\\
\frac{\hat{q}}{T^3} &= 2.6\text{–}3.3, \quad T = 486\ \text{MeV}, \text{Pb} + \text{Pb}\ 2.76\text{A TeV};\\
\frac{\hat{q}}{T^3} &= 2.5, \qquad\quad T = 516\ \text{MeV}, \text{Pb} + \text{Pb}\ 5.02\text{A TeV}.
\end{aligned} \tag{14}$$

For better visualization, we also plot the above values in Fig. 9. Also shown are the results from JET Collaboration on $\hat{q}/T^3$ for Au+Au collisions at $\sqrt{s_{\rm NN}} = 0.2$ TeV and Pb+Pb collisions at $\sqrt{s_{\rm NN}} = 2.76$ TeV. We can see that our extracted values for the scaled jet quenching parameter $\hat{q}/T^3$ are consistent with the JET Collaboration results [6].

The above analysis shows that the scaled jet quenching parameter $\hat{q}/T^3$ has some temperature dependence: it decreases as one increases the temperature, which can be understood as decreasing jet-medium interaction strength with increasing temperature. Such temperature dependence has also been found (used) in other calculations. For example, in MARTINI and MCGILL-AMY [58,71] models, jet-medium interaction strength is characterized by the strong coupling α_s. The detailed comparison to single inclusive hadron R_{AA} data renders that the averaged strong coupling at the LHC is smaller than that at RHIC [6]. Recent studies based on CUJET model [72,73] employ a Gaussian-like form for the temperature dependence of $\hat{q}/T^3$ to calculate R_{AA} and v_2 for charged hadrons.

Another interesting result is that the same $\hat{q}/T^3$ value extracted from central collisions can describe the nuclear modification data in non-central collisions reasonably well. This means that the scaled jet quenching parameter $\hat{q}/T^3$ from our study has weak dependence on the collision centrality. Such result is very similar to the finding reported in an earlier study [30] in which the scaled jet quenching parameter quantified by $K = \hat{q}/(2\epsilon^{3/4})$ shows strong dependence on the collision energy, but weak dependence on collision centrality. This puzzling result has not been fully understood yet (from our calculation). But it may be related to jet energy dependences of jet quenching parameter, which has been neglected in a lot of studies reported here.

4 Summary

In this work, we have studied the nuclear suppressions of single hadron and dihadron productions at high transverse momentum regimes in high-energy heavy-ion collisions at RHIC and the LHC. We compute the cross section of single hadron and dihadron productions in relativistic nuclear collisions based on the NLO perturbative QCD framework. For hadron production in heavy-ion collisions, we include both initial-state cold nuclear matter effect and final-state hot nuclear matter effect. The effect of jet energy loss in hot QGP medium is taken into account using medium-modified fragmentation functions, which are calculated based on the higher-twist formalism. The numerical results from our jet energy loss model calculations show consistent descriptions of the nuclear modifications of single hadron and dihadron productions in central and non-central nucleus–nucleus collisions at RHIC and the LHC.

We have further performed a detailed χ^2 analysis by comparing our jet energy loss model calculations with the experimental data on single hadron and dihadron nuclear modifications at RHIC and the LHC. From the global χ^2 analysis, we have quantitatively extracted the values of $\hat{q}_0$ for different collision systems and collision energies. For Au+Au collisions at $\sqrt{s_{\rm NN}} = 0.2$ TeV at RHIC, we obtain $\hat{q}_0 = 1.1\text{–}1.2\ \text{GeV}^2/\text{fm}$ at $T_0 = 378$ MeV (i.e., $\hat{q}/T^3 = 4.1\text{–}4.4$). For Pb+Pb collisions at $\sqrt{s_{\rm NN}} = 2.76$ TeV at the LHC, we obtain $\hat{q}_0 = 1.5\text{–}1.9\ \text{GeV}^2/\text{fm}$ at $T_0 = 486$ MeV (i.e., $\hat{q}/T^3 = 2.6\text{–}3.3$). These results are consistent with

the previous JET Collaboration results. As for Pb+Pb collisions at $\sqrt{s_{\rm NN}} = 5.02$ TeV and Xe+Xe collisions at $\sqrt{s_{\rm NN}} = 5.44$ TeV, we have used single hadron R_{AA} data to extract the $\hat{q}$ values. These extracted values are then used to predict the nuclear modification effects in dihadron productions in these collisions. Our work provides an important contribution to our quantitative extraction of the temperature dependence of jet quenching parameter by using multiple jet quenching observables from different collision systems and energies, and is helpful to achieve a consistent understanding of jet quenching in heavy-ion collisions.

Acknowledgements This work is supported in part by Natural Science Foundation of China (NSFC) under Grant nos. 11435004, 11775095, 11890711 and 11375072. SYW is also supported by the Agence Nationale de la Recherche under the project ANR-16-CE31-0019-02.

Data Availability Statement This manuscript has no associated data or the data will not be deposited. [Authors' comment: Data points used to draw the plots and predictions for the future measurements can be obtained through email upon request.]

Funded by SCOAP[3].

References

1. M. Gyulassy, M. Plumer, Phys. Lett. B **243**, 432 (1990). https://doi.org/10.1016/0370-2693(90)91409-5
2. X.N. Wang, M. Gyulassy, Phys. Rev. Lett. **68**, 1480 (1992). https://doi.org/10.1103/PhysRevLett.68.1480
3. G.Y. Qin, X.N. Wang, Int. J. Mod. Phys. E **24**(11), 1530014 (2015). https://doi.org/10.1142/S0218301315300143
4. S.A. Bass, C. Gale, A. Majumder, C. Nonaka, G.Y. Qin, T. Renk, J. Ruppert, Phys. Rev. C **79**, 024901 (2009). https://doi.org/10.1103/PhysRevC.79.024901. arXiv:0808.0908 [nucl-th]
5. N. Armesto, M. Cacciari, T. Hirano, J.L. Nagle, C.A. Salgado, J. Phys. G **37**, 025104 (2010). https://doi.org/10.1088/0954-3899/37/2/025104. arXiv:0907.0667 [hep-ph]
6. K.M. Burke et al. [JET Collaboration], Phys. Rev. C **90**(1), 014909 (2014). https://doi.org/10.1103/PhysRevC.90.014909. arXiv:1312.5003 [nucl-th]
7. Z.Q. Liu, H. Zhang, B.W. Zhang, E. Wang, Eur. Phys. J. C **76**(1), 20 (2016). https://doi.org/10.1140/epjc/s10052-016-3885-3. [arXiv:1506.02840 [nucl-th]]
8. S. Cao, T. Luo, G.Y. Qin, X.N. Wang, Phys. Lett. B **777**, 255 (2018). https://doi.org/10.1016/j.physletb.2017.12.023. arXiv:1703.00822 [nucl-th]
9. H. Zhang, J.F. Owens, E. Wang, X.N. Wang, Phys. Rev. Lett. **98**, 212301 (2007). https://doi.org/10.1103/PhysRevLett.98.212301. arXiv: nucl-th/0701045
10. H. Zhang, J.F. Owens, E. Wang, X.N. Wang, Phys. Rev. Lett. **103**, 032302 (2009). https://doi.org/10.1103/PhysRevLett.103.032302. arXiv:0902.4000 [nucl-th]
11. A. Majumder, E. Wang, X.N. Wang, Phys. Rev. Lett. **99**, 152301 (2007). https://doi.org/10.1103/PhysRevLett.99.152301. arXiv: nucl-th/0412061
12. G.Y. Qin, J. Ruppert, C. Gale, S. Jeon, G.D. Moore, Phys. Rev. C **80**, 054909 (2009). https://doi.org/10.1103/PhysRevC.80.054909. arXiv:0906.3280 [hep-ph]
13. T. Renk, Phys. Rev. C **78**, 034904 (2008). https://doi.org/10.1103/PhysRevC.78.034904. arXiv:0803.0218 [hep-ph]
14. L. Chen, G.Y. Qin, S.Y. Wei, B.W. Xiao, H.Z. Zhang, Phys. Lett. B **773**, 672 (2017). https://doi.org/10.1016/j.physletb.2017.09.031. arXiv:1607.01932 [hep-ph]
15. W. Chen, S. Cao, T. Luo, L.G. Pang, X.N. Wang, Phys. Lett. B **777**, 86 (2018). https://doi.org/10.1016/j.physletb.2017.12.015. arXiv:1704.03648 [nucl-th]
16. G.Y. Qin, B. Muller, Phys. Rev. Lett. **106**, 162302 (2011). Erratum: [Phys. Rev. Lett. **108**, 189904 (2012)]. https://doi.org/10.1103/PhysRevLett.108.189904, https://doi.org/10.1103/PhysRevLett.106.162302. arXiv:1012.5280 [hep-ph]
17. J. Casalderrey-Solana, J.G. Milhano, U.A. Wiedemann, J. Phys. G **38**, 035006 (2011). https://doi.org/10.1088/0954-3899/38/3/035006. arXiv:1012.0745 [hep-ph]
18. Y. He, I. Vitev, B.W. Zhang, Phys. Lett. B **713**, 224 (2012). https://doi.org/10.1016/j.physletb.2012.05.054. arXiv:1105.2566 [hep-ph]
19. C. Young, B. Schenke, S. Jeon, C. Gale, Phys. Rev. C **84**, 024907 (2011). https://doi.org/10.1103/PhysRevC.84.024907. arXiv:1103.5769 [nucl-th]
20. K.C. Zapp, F. Krauss, U.A. Wiedemann, JHEP **1303**, 080 (2013). https://doi.org/10.1007/JHEP03(2013)080. arXiv:1212.1599 [hep-ph]
21. X.N. Wang, Y. Zhu, Phys. Rev. Lett. **111**(6), 062301 (2013). https://doi.org/10.1103/PhysRevLett.111.062301. arXiv:1302.5874 [hep-ph]
22. N.B. Chang, G.Y. Qin, Phys. Rev. C **94**(2), 024902 (2016). https://doi.org/10.1103/PhysRevC.94.024902. arXiv:1603.01920 [hep-ph]
23. Y. Tachibana, N.B. Chang, G.Y. Qin, Phys. Rev. C **95**(4), 044909 (2017). https://doi.org/10.1103/PhysRevC.95.044909. arXiv:1701.07951 [nucl-th]
24. R. Baier, Y.L. Dokshitzer, A.H. Mueller, S. Peigne, D. Schiff, Nucl. Phys. B **484**, 265 (1997). https://doi.org/10.1016/S0550-3213(96)00581-0. arXiv:hep-ph/9608322
25. R. Baier, Y.L. Dokshitzer, A.H. Mueller, S. Peigne, D. Schiff, Nucl. Phys. B **483**, 291 (1997). https://doi.org/10.1016/S0550-3213(96)00553-6. arXiv:hep-ph/9607355
26. R. Baier, Y.L. Dokshitzer, A.H. Mueller, D. Schiff, Nucl. Phys. B **531**, 403 (1998). https://doi.org/10.1016/S0550-3213(98)00546-X. arXiv:hep-ph/9804212
27. Xf Guo, X.N. Wang, Phys. Rev. Lett. **85**, 3591 (2000). https://doi.org/10.1103/PhysRevLett.85.3591. arXiv:hep-ph/0005044
28. X.N. Wang, Xf Guo, Nucl. Phys. A **696**, 788 (2001). https://doi.org/10.1016/S0375-9474(01)01130-7. arXiv:hep-ph/0102230
29. A. Majumder, Phys. Rev. D **85**, 014023 (2012). https://doi.org/10.1103/PhysRevD.85.014023. arXiv:0912.2987 [nucl-th]
30. C. Andrés, N. Armesto, M. Luzum, C.A. Salgado, P. Zurita, Eur. Phys. J. C **76**(9), 475 (2016). https://doi.org/10.1140/epjc/s10052-016-4320-5. arXiv:1606.04837 [hep-ph]
31. C. Andrés, N. Amesto, M. Luzum, C.A. Salgado, P. Zurita, Nucl. Part. Phys. Proc. **289–290**, 105 (2017). https://doi.org/10.1016/j.nuclphysbps.2017.05.020. arXiv:1612.06781 [nucl-th]
32. C. Andres, N. Armesto, H. Niemi, R. Paatelainen, C.A. Salgado, P. Zurita, Nucl. Phys. A **967**, 492 (2017). https://doi.org/10.1016/j.nuclphysa.2017.05.115. arXiv:1705.01493 [nucl-th]
33. A. Adare et al. [PHENIX Collaboration], Phys. Rev. Lett. **101**, 232301 (2008). https://doi.org/10.1103/PhysRevLett.101.232301. arXiv:0801.4020 [nucl-ex]

34. A. Adare et al. [PHENIX Collaboration], Phys. Rev. C **87**(3), 034911 (2013). https://doi.org/10.1103/PhysRevC.87.034911. arXiv:1208.2254 [nucl-ex]
35. J. Adams et al. [STAR Collaboration], Phys. Rev. Lett. **97**, 162301 (2006). https://doi.org/10.1103/PhysRevLett.97.162301. Arxiv: nucl-ex/0604018
36. L. Adamczyk et al. [STAR Collaboration], Phys. Lett. B **760**, 689 (2016). https://doi.org/10.1016/j.physletb.2016.07.046. arXiv:1604.01117 [nucl-ex]
37. B. Abelev et al. [ALICE Collaboration], Phys. Lett. B **720**, 52 (2013). https://doi.org/10.1016/j.physletb.2013.01.051. arXiv:1208.2711 [hep-ex]
38. S. Chatrchyan et al. [CMS Collaboration], Eur. Phys. J. C **72**, 1945 (2012). https://doi.org/10.1140/epjc/s10052-012-1945-x. arXiv:1202.2554 [nucl-ex]
39. V. Khachatryan et al. [CMS Collaboration], JHEP **1704**, 039 (2017). https://doi.org/10.1007/JHEP04(2017)039. arXiv:1611.01664 [nucl-ex]
40. A.M. Sirunyan et al. [CMS Collaboration], JHEP **1810**, 138 (2018). https://doi.org/10.1007/JHEP10(2018)138. arXiv:1809.00201 [hep-ex]
41. S. Acharya et al. [ALICE Collaboration], JHEP **1811**, 013 (2018). https://doi.org/10.1007/JHEP11(2018)013. arXiv:1802.09145 [nucl-ex]
42. S. Acharya et al. [ALICE Collaboration], Phys. Lett. B **788**, 166 (2019). https://doi.org/10.1016/j.physletb.2018.10.052. arXiv:1805.04399 [nucl-ex]
43. J. Adam et al. [ALICE Collaboration], Phys. Lett. B **763**, 238 (2016). https://doi.org/10.1016/j.physletb.2016.10.048. arXiv:1608.07201 [nucl-ex]
44. K. Aamodt et al. [ALICE Collaboration], Phys. Rev. Lett. **108**, 092301 (2012). https://doi.org/10.1103/PhysRevLett.108.092301. arXiv:1110.0121 [nucl-ex]
45. R. Conway [CMS Collaboration], Nucl. Phys. A **904-905**, 451C (2013). https://doi.org/10.1016/j.nuclphysa.2013.02.046
46. T.J. Hou et al., Phys. Rev. D **95**(3), 034003 (2017). https://doi.org/10.1103/PhysRevD.95.034003. arXiv:1609.07968 [hep-ph]
47. S. Kretzer, Phys. Rev. D **62**, 054001 (2000). https://doi.org/10.1103/PhysRevD.62.054001. arXiv:hep-ph/0003177
48. X.N. Wang, Phys. Rev. C **70**, 031901 (2004). https://doi.org/10.1103/PhysRevC.70.031901. arXiv:nucl-th/0405029
49. X.N. Wang, Phys. Lett. B **595**, 165 (2004). https://doi.org/10.1016/j.physletb.2004.05.021. arXiv:nucl-th/0305010
50. X.N. Wang, Phys. Rept. **280**, 287 (1997). https://doi.org/10.1016/S0370-1573(96)00022-1. arXiv:hep-ph/9605214
51. S.Y. Li, X.N. Wang, Phys. Lett. B **527**, 85 (2002). https://doi.org/10.1016/S0370-2693(02)01179-6. arXiv:nucl-th/0110075
52. V. Emel'yanov, A. Khodinov, S.R. Klein, R. Vogt, Phys. Rev. C **61**, 044904 (2000). https://doi.org/10.1103/PhysRevC.61.044904. arXiv:hep-ph/9909427
53. T. Hirano, Y. Nara, Phys. Rev. C **69**, 034908 (2004). https://doi.org/10.1103/PhysRevC.69.034908. arXiv:nucl-th/0307015
54. K.J. Eskola, P. Paakkinen, H. Paukkunen, C.A. Salgado, Eur. Phys. J. C **77**(3), 163 (2017). https://doi.org/10.1140/epjc/s10052-017-4725-9. arXiv:1612.05741 [hep-ph]
55. C.A. Salgado, U.A. Wiedemann, Phys. Rev. D **68**, 014008 (2003). https://doi.org/10.1103/PhysRevD.68.014008. arXiv:hep-ph/0302184
56. S. Wicks, W. Horowitz, M. Djordjevic, M. Gyulassy, Nucl. Phys. A **784**, 426 (2007). https://doi.org/10.1016/j.nuclphysa.2006.12.048. arXiv:nucl-th/0512076
57. S. Jeon, G.D. Moore, Phys. Rev. C **71**, 034901 (2005). https://doi.org/10.1103/PhysRevC.71.034901. arXiv:hep-ph/0309332
58. G.Y. Qin, J. Ruppert, C. Gale, S. Jeon, G.D. Moore, M.G. Mustafa, Phys. Rev. Lett. **100**, 072301 (2008). https://doi.org/10.1103/PhysRevLett.100.072301. arXiv:0710.0605 [hep-ph]
59. A. Majumder, C. Shen, Phys. Rev. Lett. **109**, 202301 (2012). https://doi.org/10.1103/PhysRevLett.109.202301. arXiv:1103.0809 [hep-ph]
60. Wt Deng, X.N. Wang, Phys. Rev. C **81**, 024902 (2010). https://doi.org/10.1103/PhysRevC.81.024902. arXiv:0910.3403 [hep-ph]
61. E. Wang, X.N. Wang, Phys. Rev. Lett. **87**, 142301 (2001). https://doi.org/10.1103/PhysRevLett.87.142301. arXiv:nucl-th/0106043
62. E. Wang, X.N. Wang, Phys. Rev. Lett. **89**, 162301 (2002). https://doi.org/10.1103/PhysRevLett.89.162301. arXiv:hep-ph/0202105
63. N.B. Chang, W.T. Deng, X.N. Wang, Phys. Rev. C **89**(3), 034911 (2014). https://doi.org/10.1103/PhysRevC.89.034911. arXiv:1401.5109 [nucl-th]
64. H. Song, U.W. Heinz, Phys. Lett. B **658**, 279 (2008). https://doi.org/10.1016/j.physletb.2007.11.019. arXiv:0709.0742 [nucl-th]
65. H. Song, U.W. Heinz, Phys. Rev. C **77**, 064901 (2008). https://doi.org/10.1103/PhysRevC.77.064901. arXiv:0712.3715 [nucl-th]
66. Z. Qiu, C. Shen, U. Heinz, Phys. Lett. B **707**, 151 (2012). https://doi.org/10.1016/j.physletb.2011.12.041. arXiv:1110.3033 [nucl-th]
67. Z. Qiu, U. Heinz, Phys. Lett. B **717**, 261 (2012). https://doi.org/10.1016/j.physletb.2012.09.030. arXiv:1208.1200 [nucl-th]
68. X.N. Wang, Phys. Lett. B **579**, 299 (2004). https://doi.org/10.1016/j.physletb.2003.11.011. arXiv:nucl-th/0307036
69. Hz Zhang, J.F. Owens, E. Wang, X.-N. Wang, J. Phys. G **35**, 104067 (2008). https://doi.org/10.1088/0954-3899/35/10/104067. arXiv:0804.2381 [hep-ph]
70. J.G. Milhano, K.C. Zapp, Eur. Phys. J. C **76**(5), 288 (2016). https://doi.org/10.1140/epjc/s10052-016-4130-9. arXiv:1512.08107 [hep-ph]
71. B. Schenke, C. Gale, S. Jeon, Phys. Rev. C **80**, 054913 (2009). https://doi.org/10.1103/PhysRevC.80.054913. arXiv:0909.2037 [hep-ph]
72. J. Xu, J. Liao, M. Gyulassy, JHEP **1602**, 169 (2016). https://doi.org/10.1007/JHEP02(2016)169. arXiv:1508.00552 [hep-ph]
73. S. Shi, J. Liao, M. Gyulassy, Chin. Phys. C **43**(4), 044101 (2019). https://doi.org/10.1088/1674-1137/43/4/044101. arXiv:1808.05461